CARBON NANOCOMPOSITES FOR ENHANCED CATALYTIC ACTIVITIES FOR NITROPHENOL REDUCTION

***Sachin Ananda Mokal, **Dr. Kailas Narayan Sonune**

**Research Scholar, **Research Supervisor*
Faculty of Chemistry, OPJS University,
Churu, Rajasthan, India

ABSTRACT

For many uses of nanomaterials, efficient methods of production and self-assembly of nanocomposites were crucial. Herein, we report the effective synthesis of novel carbon nanotube (CNT)-Cu2O nanocomposites using a simple method. Choosing CNT as the anchoring substrate for loading Cu2O nanoparticles allowed for the fabrication of composite catalysts that were both stable and reusable. Scanning electron microscopy, energy dispersive spectroscopy, X-ray diffraction, X-ray photoelectron spectroscopy, and thermogravimetric analysis all confirmed that binary Cu/Cu2O nanocomposites (NCs) were effectively produced on Mag-S-MS without self-aggregation and oxidation. In further research, it was tested as a catalyst for the hydrogenation-based reduction of 4-NP to 4-aminophenol (4-AP) using NaBH4 as the reducing agent. It was studied how much of a catalyst was used, as well as how much NaBH4 and 4-NP were present at the outset. After 4 hours of contact time, at pH 7, the catalytic activity of investigated materials was greater than under acidic and basic environments, resulting in degradation rates of up to 93%. The highest catalytic characteristics were found in an amorphous iron hydroxide with a Zr/Fe molar ratio of 75%:25%. As an alternative to traditional methods of combating organic compound-induced water pollution, these cutting-edge materials hold considerable promise.

Keywords: *Nanocomposite, Cuprous oxide, Carbon nanotube, Catalytic reduction, P-nitrophenol*

INTRODUCTION

Carbon nanotubes (CNT) have sparked a flurry of investigation into their potential as catalysts, flexible supercapacitors, electronic sensors, and a sustainable means of wastewater treatment. CNTs have been recognised as exceptional materials because to their great chemical stability, good electrical conductivity, enormous specific surface area, and tremendous mechanical strength. Due to their unique characteristics, CNTs are a boon to scientific inquiry. Research on CNT catalysis has increased in recent years, with most studies focusing on composites using transition metals. For instance, Karimi-Maleh et al. have created CuO/CNTs nanocomposite as high sticky carbon paste electrode using chemical precipitation approach. Since nanoscience and nanotechnology have recently advanced, it has become crucial to devise a simple and inexpensive method of producing multi-functional carbon material. Simultaneously, a wide variety of nanomaterials, including Pd, TiO, Mo, Zn, Au, and Ag,

have been the subject of study with the aim of enhancing catalytic capabilities. To aid photoenzymatic reaction in sustainable fuel synthesis, Liu et al. employed zinc to create chloroplast mimics using the self-assembled technique. For instance, because to their high reactivity and selectivity, silver nanoparticles are increasingly being employed as catalysts. Pt nanoparticles also have the potential to act as an electron separator. Selfmineralization of Pt and TiO2 reorganised the architecture of the fiber bundles.

Peptide-porphyrin co-assemblies were studied, and the results included readily mineralized Pt nanoparticles given by Liu et al. Li and colleagues prepared a dendritic pyrenyl-moiety-decorated hyperbranched polyglycidol (pHBP) to functionalize CNTs in a non-covalent (non-destructive) manner; subsequent in situ deposition of Au, Ag, and Pt nanoparticles with uniform SiO2, GeO2, and TiO2 coatings on the as-prepared CNT/pHBP hybrids completed the process. Excellent catalytic activity for 4-NP reduction was found for novel CNT/pHBP/Au and CNT/pHBP/Pt hybrids. In addition, Szekely's team produced outstanding work concerning an azido-derivatized cinchona-squaramide bifunctional catalyst grafted to the surface of a polybenzimidazole-based nanofiltration membrane, providing further confirmation of the change in geometry, an increase in secondary interactions, and a consequent improvement in the catalytic effect. Copper nanocrystals, on the other hand, were a part of the group of catalytic materials that were both cheap and plentiful. The catalytic outcomes were also determined by the surface microstructures and the arrangement of the Cu atoms on the surface, in addition to the size and shape. The capacity of Cu+ salts to accelerate a cycloaddition process at room temperature or under mild heating was investigated by Meldal and Sharpless. Electrocatalysis, photocatalysis, and CO2 catalysis were all greatly aided by the incorporation of functionalized Cu catalysts into Cu nanoparticles. There have been reports of Cu's use in visible light active photocatalyst applications, for instance.

Successful photocatalytic CO2 reduction and functionalization of Cu and Cd catalysts were achieved in that study. Catalytic oxidation processes using copper nanostructures have also been performed, however their underlying mechanisms vary from those of other metal catalysts. Many scientists have used CNTs as templates to support heterogeneous catalysts because to their hydrophobicity, unique nanostructure, high mechanical strength, high thermal and electrical conductivity, and high adsorption. High enzyme wiring efficiency and electron transfer rate were observed in hybrid nanoflower composites using CNTs, suggesting their potential use in the area of constructing enzymatic biofuel cells.

While Esumi's team investigated dendrimer-encapsulated Au NPs for 4-NP reduction, they found that the process was sensitive to dendrimer concentration and production. Similarly, there have been reports of studies with CNT and Cu composites. Using the CVD technique and electrodeposited with CNT, Leggiero et al. typically reported good conductors in the seeded Cu. In situ production of CNT and metal matrix composites of chromium carbide was investigated by Cho et al., leading to the achievement of incompatible features such as electrical conductivity and temperature coefficient of

resistance. Here, we detail a straightforward method for manufacturing stable CNT-Cu2O nanocomposites. The CuCl precursor was converted into Cu2O nanocrystals. We controlled the sizes of the produced Cu nanostructures by adjusting the preparation temperatures and times. Preparation in this instance seemed easy, environmentally friendly, and low-cost in comparison to the procedure provided in the last study. In addition, the as-prepared composite materials may be put to use as novel catalytic materials in the reduction process of 4-nitropyridine. In particular, our research may find useful applications in the areas of wastewater treatment and composite catalytic materials.

LITERATURE REVIEW

Anita Cymann-Sachajdak (2020) The function of oxidised carbon nanotubes in poly-3,4-ethylenedioxytiophene (PEDOT)/graphene oxide composite is reported here. Monomer, oxidised carbon nanotubes, and graphene oxide are suspended in a solvent, and the ternary composites are synthesised by electrodeposition. On the surface of graphene oxide, dissociated functional groups serve as counter-ions for the polymer chains. The research provides a thorough analysis of the ternary composites, including their physicochemical and electrochemical properties. The findings show that the capacitance values of the ternary composites are twice those of the binary composites due to the inclusion of oxMWCNTs. The physicochemical features of the composites, their adherence to the electrode substrate, and their electrochemical performance are all very sensitive to the concentration of carbon nanotubes in the synthesis fluid.

AgataFedorczyk (2017) On a glassy carbon electrode, a simple electrochemical/chemical approach was used to create an organic-inorganic hybrid system consisting of bimetallic Au@Pt nanoparticles with a diameter of a few nanometers evenly disseminated in the conducting polymer matrix. Improved specific catalytic activity (9.7 A mg1 Pt) is shown in the electrooxidation of formic acid using the refined catalyst. The polymer structure utilised as the matrix for the bimetallic catalyst and the process of production of Au@Pt nanoparticles are examined in terms of their roles in the enhanced performance. The effect of synthesis circumstances on the parameters of the catalyst is investigated by comparing the electrocatalytic activity of hybrid systems generated via two distinct methods. HR-TEM, X-ray diffraction, and X-ray fluorescence are used to characterize the composites. EDX elemental mapping is used to figure out the nanoparticle arrangement in Au@Pt composite. It is suggested that thin polymer films be used to insert samples prior to XRD and XRF analysis.

Sylwia Zoladek, (2016) It has been shown that Co-porphyrin catalytic centres may be actively supported by three-dimensional multi-layered films (on glassy carbon) made of networks of polyoxometallate (PMo12O40 3)-modified gold nanoparticles connected together by the alternately produced ultra-thin layers of polypyrrole. In order to create hybrid organic-inorganic films (supports), a layer-by-layer method has been used. The stabilising effect and the ease of diffusion of Au nanostructures are due to the attraction of polyanionic (phosphomolybdate) adsorbates on gold nanoparticles by positively charged sites of conducting polymer (polypyrrole) structures. Scanning

electron microscopy, in addition to chronoamperometric and voltammetric methods, have been used to characterise the systems. Significant electrocatalytic enhancement effects (voltammetric current increases) have been observed in the electroreduction of oxygen in acid medium by supporting Co-porphyrin centres onto the hybrid film of the polymer-linked phosphomolybdate-stabilized gold nanoparticles. This is in comparison to the standard response of the simple porphyrin deposit on glassy carbon measured under similar conditions. Hydrogen peroxide's reductive breakdown to water is a major problem, and the hybrid film (support) itself is quite active in this process. The O2 reduction process is likely to begin at Co-porphyrin catalytic sites (two-electron reduction to H2O2) and continue (two-electron reduction to H2O) at the hybrid film containing gold nanoparticles dispersed within the highly porous cauliflower-like structures of polypyrrole multi-layers, which is essential to the system's performance. Non-covalent - interactions of porphyrin rings with polypyrrole interlayers and charge transfers between negatively charged (PMo12O40 3 modified) gold nanoparticles and positively charged nitrogen sites of polypyrrole may also contribute to synergy in charge distribution within the hybrid electrocatalytic film.

K.J.Dunst (2018) The authors of this study used in-situ Raman spectroscopy to learn more about the NO2 reaction process with the PEDOT-RGO composite film. Electrodeposition was utilised to create thin films of reduced graphene oxide (RGO), poly(3,4-ethylenedioxytiophene)-reduced graphene oxide (PEDOT-RGO), and poly(3,4-ethylenedioxytiophene)/ClO4 (PEDOT/ClO4), which were tested as resistance sensors for detecting nitric oxide gas. Increasing resistance and an irreversible reaction were seen in experiments with NO2, suggesting that this gas overoxidizes the PEDOT polymer (PEDOT/ClO4 film). However, the reaction of PEDOT-RGO to NO2 may be reversed. In the case of a brief exposure to NO2, the PEDOT in the PEDOT-RGO composite does not react to the gas, while the presence of RGO in the composite has no effect on the overoxidation potential. The nitrogen dioxide interacts more quickly with the reduced graphene oxide, therefore the RGO "protects" the polymer from the harmful overoxidation process.

Halima Djelad, (2018) On glassy carbon (GC) electrodes, silica-modified hybrid materials were produced by electroassisted deposition of sol-gel precursors. As a means of improving the inorganic matrix's electrochemical performance, single-wall carbon nanotubes (SWCNTs) were disseminated in a silica matrix (SWCNT@SiO2). The ferrocene redox probe was used to examine the composite electrodes' electrochemical performance. When compared to ferrocene, the electrochemical performance of SWCNT@SiO2 is superior. After successfully synthesising a composite of poly(3,4-Ethylendioxythiophene)-poly(sodium 4-styrenesulfonate) (PEDOT-PSS) and silica via reactive electrochemical polymerization of the precursor EDOT in aqueous solution, it was found that the insertion of PEDOT-PSS into the silica matrix increases the heterogeneous rate constant of the SWCNT@SiO2. Heterogeneous rate constants were almost three times as high for the SWCNT@SiO2-PEDOT-PSS composite electrodes as they were for the electrode without conducting polymer. Also, compared to SWCNT@SiO2-modified electrodes, the electroactive area is more than twice as large. Scanning electron microscopy was used to examine the film samples for morphology.

MATERIALS AND METHODS

Materials

Dalian, China, was the source of the maize straw. It was then chopped into 5 cm length pieces and treated with 10% NaOH for 2 hours at 25 °C. The alkalized material was neutralised by washing it with deionized water and then oven-dried at 80 °C. The obtained solid was broken into fragments between 50 and 500 m in size. The stock Cu(II) solution was made by adding a specific quantity of CuSO4 5H2O to 100 mL of distilled water. All of the compounds were of analytical quality and were utilised in their purified forms.

Preparation of S-MS

For the synthesis of S-MS, the chemical procedure used was (Guo et al. 2015). First, 50 mL of xylene was combined with 1.0 g of succinic anhydride and 0.5 g of MS. The reaction mixture was then supplemented with 1.4 mL of triethylamine and allowed to reflux for 8 hours. Ethanol and water were used to filter and wash the resulting solid.

Preparation of amine-functionalized magnetic nanoparticles

Solvothermal preparation of NH2-Fe3O4 (Wang et al. 2006). A clear solution was obtained by dissolving 3.0 g FeCl3 6H2O, 2.0 g anhydrous sodium acetate, and 6.5 g 1,6-hexanediamine in 30 mL of ethylene glycol and rapidly stirring the mixture at 50 °C for 30 minutes. The mixture was placed in a stainless-steel autoclave with a 50 mL Teflon liner and heated to 198 degrees Celsius for 6 hours. We used water and ethanol to clean the items before drying them in a vacuum at 50 degrees Celsius.

Preparation of Mag-S-MS and Mag-NaS-MS

In order to activate the carboxylic acid functions, 1g S-MS (5.8 mmol/g) and a specific quantity of N,N′-diisopropylcarbodiimide (DIC) were added to a three-neck flask containing 50 mL dimethylformamide (DMF) and agitated at 30 °C for 2 hours. After 15 hours of stirring, 0.3 g of NH2-Fe3O4 was added to the reaction. Deionized water and 95% ethanol were used to clean the resultant black solid after magnetic decantation had separated it. The substance was desiccated overnight to preserve its stability and was given the trade name Mag-S-MS. The alkalization procedure was used to make Mag-NaS-MS. For 2 hours at 25 2 °C, Mag-S-MS was blended with 0.01 mol/L of sodium carbonate solution. Deionized water was used to wash the product until the pH of the effluent remained unaffected. Mag-NaS-MS sample dried in vacuum at 50 °C.

Fabrication and catalytic performance of Cu/Cu2O NCsloaded-Mag-S-MS

Mag-NaS-MS and Cu(II) solution (100 mg/L) were shaken for 2 hours at 25 2 °C on a thermostat water-wash shaker (SHZ-82 A, China) at a speed of 150 rpm. Cu 2+ loaded Mag-SMS was agitated with 1M NaBH4 for 2h on a thermostat water-wash shaker, and then washed many times with ultra-pure water to eliminate any free Cu 2+. In order to catalyse the reduction of 4-NP, a combination of 0.3 mL of 4-NP (5 10 4 M), 1.2 mL of 0.01 M NaBH4, and 1.5 mL of ultrapure water was placed in a quartz cell and stirred. The mixture was catalysed by adding a certain quantity of Cu/Cu2O NCs loaded with Mag-S-MS. UV-Vis spectrophotometer (VARIAN, SCAN-50) readings were taken of the catalytic process from 250 to 500 nm. Observing the fade in the 400 nm absorption peak's intensity over time allowed us to calculate the rate constant (k). To investigate the catalyst's reusability, a black solid was separated using a portable magnet. In the same reaction system, it was utilised repeatedly after being rinsed with sterile water.

Characterization and measurements

The FTIR spectrum was used to characterise the functional groups in Mag-S-MS (Perkin-Elmer, USA). All of the specimens' surface morphologies were acquired using an energy dispersive X-ray spectrometer attached to a field emission SEM (JSM-6460, JEOL, Japan) (Oxford, British). Shimadzu XRD-6100 diffraction patterns were obtained from 5o to 80o using CuK radiation (= 1.54060). All samples were analysed for their magnetic characteristics using a Lake Shore 7410 VSM in a room temperature environment. Under a stream of nitrogen, a thermogravimetric analysis was conducted from 25 to 600 degrees Celsius at a heating rate of 10 degrees Celsius per minute. An Al-Ka X-ray source was used in an X-ray photoelectron spectrometer (XPS) to take the XPS and XAES readings on Page 5/23. (1486.6 eV).

RESULTS AND DISCUSSION

Characterization of Catalysts.

Figure 2 shows the X-ray diffraction patterns of the tested materials. Assigning these peaks to the various iron (oxy)hydroxides, they were found to be positioned between 2 and 20 degrees. Specifically, -FeOOH and HFO showed concentrations of 8-11%. It is important to note that these results corroborated those found by other writers. All XRD patterns had two peaks in the 2 ranges of 15° -40° and 40° -70°, suggesting an amorphous solid state [33]. According to JCPDS No. 42-1164, zirconia was discovered to reside mostly in the monoclinic phase, with only a very minor peak connected to the tetragonal phase. XRD analysis also revealed that the peaks in the diffraction pattern of HFO and FeOOH-based materials that were present in the raw feedstock disappeared, whereas peaks associated to goethite at 2 = 22, 34, and 37° were more prominent. The previous catalyst's XRD pattern included peaks at 2 = 28:5 and 31.8, showing that it still contained zirconium in its monoclinic phase. However,

water was present in the catalyst, which is likely what caused the monoclinic phase of zirconia to disappear. The average particle size of iron oxide aggregates was calculated to be between 25 and 34 nm using the Debye-Scherrer equation. Figure 3 displays the reported FTIR spectra of the tested catalysts. Bands at 4000 and 3630 cm1 (broad) and 1630 up to 1480 cm1 (weak) are indicative of (oxy) iron hydroxides, and their presence is linked to the coexistence of zirconium and ferric (oxy)hydroxides (small). It was determined that the absorption band at 1635 cm-1, which was ascribed to the deformation vibrations of H2O molecules, was associated with the (oxy)hydroxides. The spectral band at 3625 cm-1 in goethite was identified as the OH bond vibration.

The faint absorption band at 837 cm-1 was ascribed to the Zr-O stretching mode, while the stronger absorption bands at 3320 and 1640 cm-1 were related to the asymmetric stretching and bending modes of OH groups. Table 3 lists the BET surface areas for each material. The HFO-based catalysts had greater average specific surface areas than the goethite catalysts. Take note that the oxidation reaction findings for the catalysts produced with HFO and zirconium might be partly explained by this textural property. The N2 adsorption desorption isotherm of the catalyst 25HFe75Zr at 77 K is shown in Figure 4. Type IV in the IUPAC classification, this isotherm is indicative of monolayer adsorption in the presence of mesopores. The sample has a calculated BET surface area of 267.66 m2/g and a pore volume of 0.262 cm3/g. The shape of the supports, the presence of grains, and the porosity in the goethite and HFO-based catalysts were all analysed using SEM images. Figure 5 shows a scanning electron micrograph (SEM) picture of goethite and HFO, which reveals that these (oxy)hydroxides exist as a precipitate and have relatively opaque and nonregular structures (a). It was also discovered that catalyst samples of varying compositions had a regular and ordered shape, with spherical-like morphologies. See Figure 5 for the elemental analysis findings, which verified the presence of iron, zirconium, and trace amounts of silica and aluminium in the examined materials (b). The powder PZC values varied from 4.11 to 10.42 and the grain PZC values from 6.07 to 11.12, as shown in Table 4. PZC, as stated, is the pH value at which a solid's net surface charge is zero. The solution's pH determines whether a solid's surface charge is positive, negative, or neutral. The surface charge of the substance is positive at pH PZC and negative for pH > PZC. Therefore, this feature aids in deciphering the impact of solution pH on pollutant degradation and provides insight into phenomena that may occur throughout the catalytic process. The results of the grains' mechanical testing are summarised in Table 5. All of the grains had a compaction capacity in the range of 5–17 mL, which is in line with typical values (European pharmacy). Grain catalysts had a friability of less than 1%.

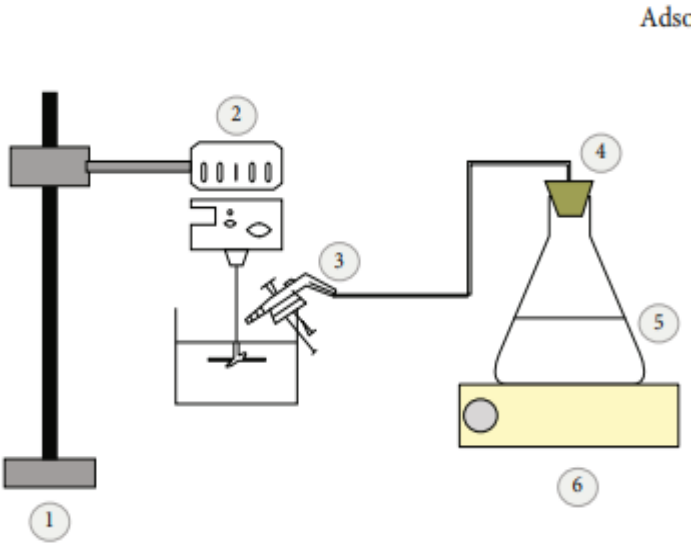

Figure 1: Configuration of mixer granulator used in the preparation of catalyst for the degradation of 4-nitrophenol. (1) Support, (2) mechanical stirrer, (3) sprayer, (4) plug, (5) Erlenmeyer flask, and (6) magnetic stirrer.

Table 2: Operating conditions used in the granulation process of Catalyst

Mass of the powder, g	20
Rotation speed of the studied mixer, rpm	100 to 1000
Concentration of the binder solution, %	40
Duration of the process, min	6

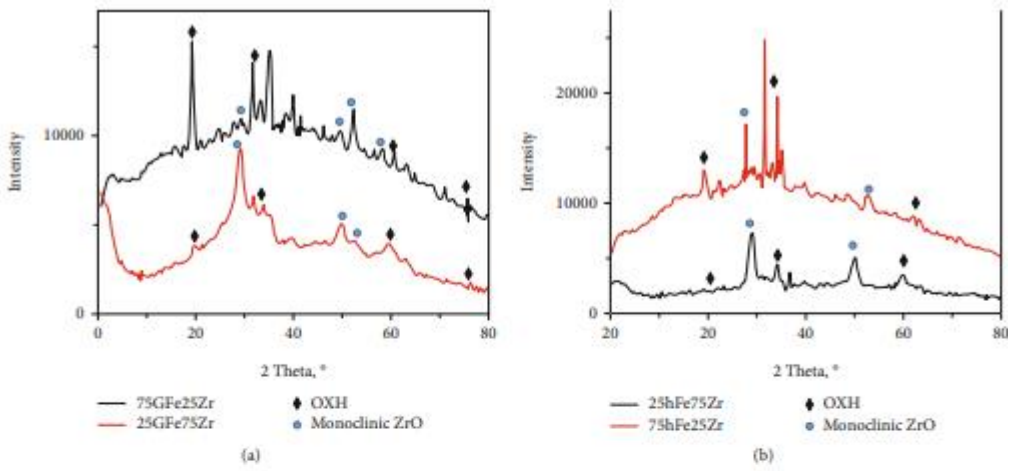

FIGURE 2: X-ray diffraction patterns of catalyst samples used in the degradation of 4-nitrophenol.

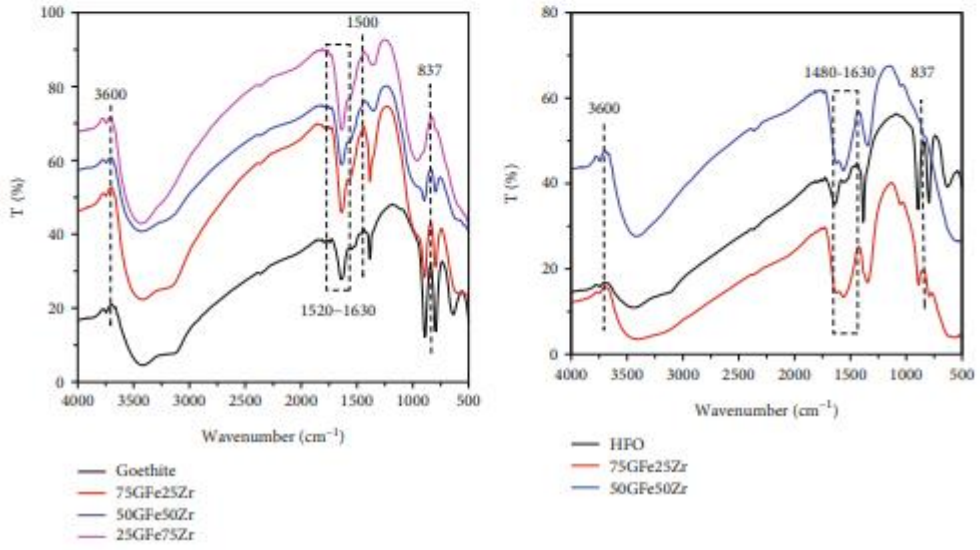

Figure 3: FTIR spectra of catalyst samples used in the degradation of 4-nitrophenol.

Table 3: Main textural parameters of catalysts prepared in this study.

Sample	BET surface area, m^2/g	Pore volume, cc/g
75HFe25Zr	213.911	0.159
50HFe50Zr	236.418	0.2567
25HFe75Zr	267.661	0.261
50GFe50Zr	232.551	0.1682
75GFe25Zr	114.809	0.12
25GFe75Zr	188.496	0.1464

Modifications to the 4-NP Degradation Caused by Operating Conditions. Figure 6 displays the findings of the influence of contact time on the 4-NP conversion rate (a).

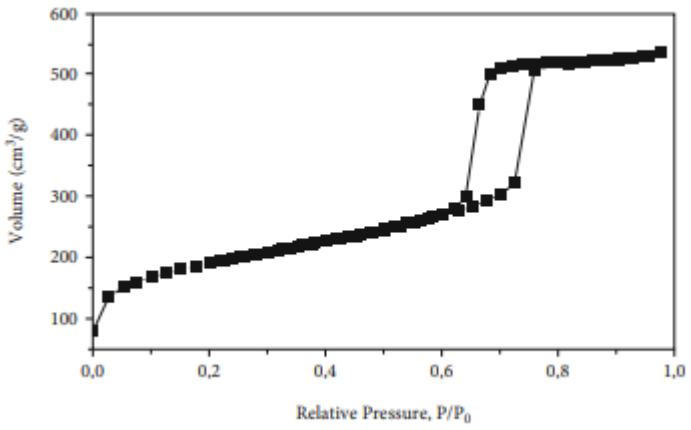

Figure 4: N2 adsorption-desorption isotherms at 77 K of catalyst sample 25HFe75Zr.

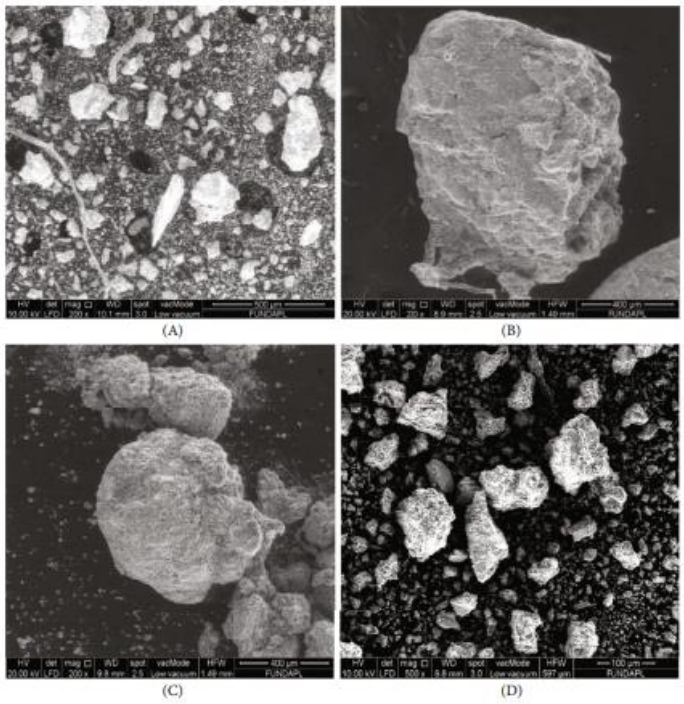

CONCLUSIONS

In conclusion, we have introduced a simple and inexpensive technique for synthesising CNT-Cu2O nanocomposites. The current CNT-Cu2O composite was synthesised at 30 °C for 1 h, which, as determined by extensive analysis, produced Cu2O particles of a size between 30 and 50 nm that were evenly dispersed throughout the CNT surface. The reduction process may be sped up by adding more catalyst and NaBH4, whereas adding more 4-NP has the reverse effect. The catalyst's super-paramagnetism makes it simple to extract it from the solution using a magnetic field. When tested for

reusability, catalysts exhibited little to no loss of activity after being recycled five times. Catalytic experiments demonstrated that zirconium-supported HFO-synthesized grains were effective in degrading 4-nitrophenol in a neutral medium. Catalysts based on hydrofluorooctanoic acid (HFO) are useful tools for removing organic molecules from wastewater.

REFERENCES

1. Cymann-Sachajdak, Anita & Sawczak, Miroslaw & Ryl, Jacek & Klugmann-Radziemska, Ewa & Wilamowska-Zawłocka, Monika. (2020). Capacitance Enhancement by Incorporation of Functionalised Carbon Nanotubes into Poly(3,4-Ethylenedioxythiophene)/Graphene Oxide Composites. Materials. 13. 2419. 10.3390/ma13102419.

2. Fedorczyk, A.; Pomorski, R.; Chmielewski, M.; Ratajczak, J.; Kaszkur, Z.; Skompska, M. Bimetallic Au@Pt nanoparticles dispersed in conducting polymer—A catalyst of enhanced activity towards formic acid electrooxidation. Electrochim. Acta 2017, 246, 1029–1041, doi:10.1016/j.electacta.2017.06.138.

3. Zoladek, S., Rutkowska, I.A., Blicharska, M. et al. Enhancement of oxygen reduction at Co-porphyrin catalyst by supporting onto hybrid multi-layered film of polypyrrole and polyoxometalate-modified gold nanoparticles. J Solid State Electrochem 20, 1199–1208 (2016). https://doi.org/10.1007/s10008-016-3135-5

4. Dunst, K.J.; Trzciński, K.; Scheibe, B.; Sawczak, M.; Jasiński, P. Study of the NO2 sensing mechanism of PEDOT-RGO film using in situ Raman Spectroscopy. Sens. Actuators B Chem. 2018, 260, 1025–1033, doi:10.1016/j.snb.2018.01.089

5. Djelad, H.; Benyoucef, A.; Morallón, E.; Montilla, F. Reactive insertion of PEDOT-PSS in SWCNT@silica composites and its electrochemical performance. Materials (Basel) 2020, 13, 1200, doi:10.3390/ma13051200.

6. Gierwatowska, M.; Kowalewska, B.; Cox, J.A.; Kulesza, P.J. Multifunctional mediating system composed of a conducting polymer matrix, redox mediator and functionalized carbon nanotubes: Integration with an enzyme for effective bioelectrocatalytic oxidation of glucose. Electroanalysis 2013, 25, 2651–2658, doi:10.1002/elan.201300423.

7. Lisowska-Oleksiak, A.; Wilamowska, M.; Jasulaitiené, V. Organic–inorganic composites consisted of poly(3,4-ethylenedioxythiophene) and Prussian Blue analogues. Electrochim. Acta 2011, 56, 3626–3632, doi:10.1016/j.electacta.2010.12.092.

8. Adamczyk, L.; Kulesza, P.J. Fabrication of composite coatings of 4-(pyrrole-1-yl) benzoate-modified poly3,4-ethylenedioxythiophene with phosphomolybdate and their application in

corrosion protection. Electrochim. Acta 2011, 56, 3649–3655, doi:10.1016/j.electacta.2010.12.078.

9. Skompska, M. Hybrid conjugated polymer/semiconductor photovoltaic cells. Synth. Met. 2010, 160, 1–15, doi:10.1016/j.synthmet.2009.10.031.

10. Ningsih, P.; Holdsworth, C.Z.; Donne, S.W. The Initial Study of Polyaniline with Manganese Oxides for Electrochemical Capacitors. Procedia Chem. 2015, 16, 540–547, doi:10.1016/j.proche.2015.12.090.

11. Bryan, A.M.; Santino, L.M.; Lu, Y.; Acharya, S.; D'Arcy, J.M. Conducting Polymers for Pseudocapacitive Energy Storage. Chem. Mater. 2016, 28, 5989–5998, doi:10.1021/acs.chemmater.6b01762.

12. Snook, G.A.; Kao, P.; Best, A.S. Conducting-polymer-based supercapacitor devices and electrodes. J. Power Sources 2011, 196, 1–12, doi:10.1016/j.jpowsour.2010.06.084.

13. Snook, G.A.; Peng, C.; Fray, D.J.; Chen, G.Z. Achieving high electrode specific capacitance with materials of low mass specific capacitance: Potentiostatically grown thick micro-nanoporous PEDOT films. Electrochem. Commun. 2007, 9, 83–88, doi:10.1016/j.elecom.2006.08.037.

14. Das, P.R.; Grafenstein, A.; Ledwoch, D.; Osters, O.; Komsiyska, L.; Wittstock, G. Conducting Polymers as Binder Additives for Cathodes in Li Ion Battery. ECS Trans. 2014, 63, 31–43, doi:10.1149/06301.0031ecst.

15. Das, P.R.; Komsiyska, L.; Osters, O.; Wittstock, G. PEDOT: PSS as a Functional Binder for Cathodes in Lithium Ion Batteries. J. Electrochem. Soc. 2015, 162, A674–A678, doi:10.1149/2.0581504jes.